ELSEVIER

Biochimica et Biophysica Acta 1234 (1995) 235–243

BBA Biochimica et Biophysica Acta

Acyl chain length dependence in the stability of melittin-phosphatidylcholine complexes. A light scattering and ^{31}P-NMR study

Jean-François Faucon, Jean-Marc Bonmatin, Jean Dufourcq, Erick J. Dufourc *

Centre de Recherche Paul Pascal, CNRS, Avenue Albert Schweitzer, 33600 Pessac, France

Received 27 July 1994; accepted 24 November 1994

Abstract

Light scattering and ^{31}P-NMR have been used to monitor the effect of the bee-toxin, melittin, on phosphatidylcholine (PC) bilayers of variable acyl chain length (from $C_{16:0}$ to $C_{20:0}$). Melittin interacts with all lipids provided the interaction is initiated in the lipid fluid phase. For low-to-moderate amounts of toxin (lipid-peptide molar ratios, $R_i \geq 15$), the system takes the form of large spheroidal vesicles, in the fluid phase, whose radius increases from 750 Å with dipalmitoyl-PC (DPPC) to 1500 Å with diarachinoyl-PC (DAPC). These vesicles fragment into small discoids of 100–150 Å radius when the system is cooled down below T_c (the gel-to-fluid phase transition temperature). Little chain length dependence is observed for the small objects. Small structures are also detected independently of the physical state of lipids (gel or fluid) when $R_i \leq 5$ and provided the interaction has been made above T_c. Small discs clearly characterized for DPPC and distearoyl-PC (DSPC) lipids are much less stable with DAPC. However in the long term, all these small structures fuse into large lipid lamellae. Discs are thermodynamically unstable and kinetics of disappearance of the small lipid-toxin complexes increases as the chain length increases in the sense: DAPC ≫ DSPC > DPPC. Kinetics of fusion of the small discs into extended bilayers is described by a pseudo-first-order law involving a lag time after which fusion starts. Increasing the chain length decreases the lag time and increases the rate of fusion. Formation of both the large vesicles in the fluid phase and the small discs in the gel phase as well as their stability is discussed in terms of relative shapes and dynamics of both lipids and toxin.

Keywords: Melittin; Model membrane; Phosphatidylcholine chain length; Light scattering; NMR, ^{31}P-

1. Introduction

Melittin, the bee venom toxin, has been recently shown to promote considerable modifications in the structure and dynamics of model membranes. Several biophysical techniques such as deuterium (^{2}H) and phosphorus (^{31}P)-NMR, light scattering, electron microscopy, fluorescence, afforded a converging view regarding the mode of action of this toxin on model membranes [1–5]. It appears that melittin restructurates, by fusion or fragmentation the model membranes to form new entities (lipid-toxin complexes) whose size and shape depend on the physical state of the lipids and on the lipid-to-toxin molar ratio, for a review see [6]. This mode of action which has been well documented for DMPC and DPPC membranes seems to be applicable to a certain extent to natural [7] and real membranes [8–10]. However, the relative importance of the structural parameters of the real membrane (lipid chain length and the degree of unsaturation, nature and charge of the head group, presence of cholesterol and proteins) must be well determined in order to depict at the molecular level the mode of action of melittin on real cells, on the basis of molecular mechanisms evidenced on model systems.

It has been shown that model membrane restructuration occurs at the temperature of the gel-to-fluid phase transition, T_c [3] of the pure lipid membrane. The transition from very small discs (ca. 200 Å diameter) observed in the fluid

Abbreviations: QELS, quasi-elastic light scattering; NMR, nuclear magnetic resonance; TLC, thin-layer chromatography; DLPC, 1,2 dilauroyl-*sn*-glycero-3-phosphorylcholine; DMPC, 1,2-dimyristoyl-*sn*-glycero-3-phosphorylcholine; DPPC, 1,2-dipalmitoyl-*sn*-glycero-3-phosphorylcholine; DSPC, 1,2-distearoyl-*sn*-glycero-3-phosphorylcholine; DAPC, 1,2-diarachinoyl-*sn*-glycero-3-phosphorylcholine; $C_{12:0}$, lauric acid; $C_{14:0}$, myristic acid; $C_{16:0}$, palmitic acid; $C_{18:0}$, stearic acid; $C_{20:0}$, arachidic acid; T_c, gel-to-fluid phase transition temperature; R_H, hydrodynamic radius; R_i, lipid-to-peptide molar ratio.

* Corresponding author. Fax: +33 56 845600.

SSDI 0005-2736(94)00298-3

phase, appears to be triggered by the cooperative melting of the lipid acyl chains. The size and shape transition is reversible with DMPC and DPPC, that is to say, one can induce fragmentation of the large vesicles by simply decreasing the temperature of the system from fluid to gel phases, or fusion of the small discs by increasing the temperature from low ($T < T_c$) to high temperatures ($T > T_c$). Interestingly, this phenomenon can only be observed when the system has been brought once above T_c [11], i.e., melittin does not form small discs when directly added to lipids multilayers in their gel phase [2]. This leads to believe that the small structures formed below T_c are metastable [5].

The aim of the present work is to investigate on the stability of melittin-lipid complexes and to monitor how lipid chain length modulates both the formation and the stability of these small structures. Three techniques will be used to monitor membrane changes both at the macroscopic (light scattering, quasi elastic light scattering) and molecular (^{31}P-NMR) levels. It will be described herein that the fusion and fragmentation mechanisms already reported can be generalized from $C_{14:0}$ to $C_{20:0}$ phosphatidylcholine membranes. The stability of the small toxin-lipid complexes will be shown to strongly depend on acyl chain length and to reach a threshold with DAPC for which discs are barely detected.

2. Materials and methods

Phosphatidylcholines of variable chain length were either synthesized according to already published procedures [12] or purchased from Sigma (St. Louis, MO). Melittin was obtained from Bachem (Switzerland) and used without further purification. Model membranes were obtained by hydrating lipids with a buffered solution (200 mM Tris, 2 mM EDTA, 100 mM NaCl, pH 7.5) and gentle shaking on a vortex mixer at $T > T_c$. In order to ensure membrane homogeneity, several freeze-thaw cycles were performed. Melittin dissolved in the same buffer solution was added to bilayers at the desired lipid-to-toxin molar ratio R_i. The mixture was then incubated 30 min above T_c prior starting any measurements. Phospholipid concentrations varied according to techniques; typical values were 0.1–1 mM for light scattering and 50 mM for NMR. Phospholipid degradation was checked by TLC. Lysophosphatidylcholine (ca. 5%) was only detected after long run experiments (several days) in which repeated cooling and heating cycles had been performed. Temperature quenches, when needed, were performed as follows: the measuring cell was equilibrated at a temperature below T_c and the sample, incubated above T_c, was placed into the cell as quickly as possible. The time estimate for the sudden temperature decrease is about 10–20 s.

Light scattering experiments were performed on a home-made apparatus allowing computer-driven data acquisition and temperature scans to $\pm 1°$ C [13]. The excitation wavelength was set to 480 nm and the scattered intensity recorded at 90° with respect to the incident beam. QELS measurements were carried out by means of a krypton ion laser source ($\lambda = 647$ nm, Spectra Physics). The correlation function of the scattered light was recorded at 90° and fast clipped on a 100-channel detector (ANTE, Paris) with a time resolution of 10 ns. The method of Mazer et al. [14] was used to sample the correlation function over three orders of magnitude in time. Temperature was controlled to $\pm 0.2°$ C.

Phosphorus-31 (^{31}P)-NMR was performed on a Bruker WH 270 spectrometer implemented for solid state measurements and operating at 109.35 MHz. NMR data were recorded by means of the Hahn-echo pulse sequence [15]. Gated broad proton decoupling was utilized during acquisition and temperature was controlled to $\pm 1°$ C. Data treatment was accomplished on a VAX/VMS 8600 computer. Correlation times and hence hydrodynamic radii were extracted from QELS data by means of one-or two exponential functions (Faucon, unpublished data). NMR spectral moments were calculated according to Abragam [16] and by defining the zero of frequencies at the isotropic chemical shift position. This value was taken on samples with very large isotropic lines and kept constant for the entire temperature series on a given sample.

3. Results

3.1. Light scattering

The gel-to-fluid phase transition temperature of pure lipid dispersions may be detected by light scattering (data not shown). A sudden increase in turbidity, leading to a greater light scattering, when decreasing the temperature through T_c allows to find that T_c (DPPC) = 41° C, T_c (DSPC) = 54° C, T_c (DAPC) = 66° C in accordance with the literature [17]. These transition temperatures are indicated in Fig. 1 by dashed lines. This figure reports the thermal variation of the light scattered intensity for three model membrane systems (DPPC, DSPC and DAPC), in the presence of melittin ($R_i = 15$). Experiments were performed by decreasing the temperature very slowly (5° C/h) from fluid phase temperatures. The most noticeable phenomenon is that the light scattered intensity severely decreases on going into the gel phase for DPPC and DSPC model membranes whereas the converse is observed for DAPC, i.e., the fluid-to-gel transition region is associated with a net turbidity increase. For the three systems, the abrupt change occurs at about the gel-to-fluid phase transition temperature. In addition, far away from either side of T_c, the intensity reaches a plateau where it remains almost constant. Both DPPC- and DSPC-melittin profiles are qualitatively comparable; however, it is noteworthy that the scattered intensity at the plateau, both below and above

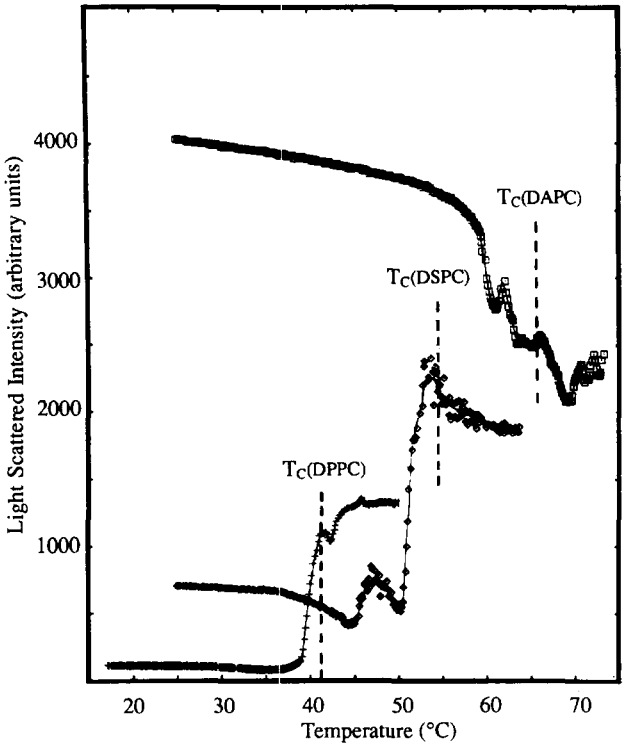

Fig. 1. Temperature dependence of the light scattered intensity for DPPC (+), DSPC (◇) and DAPC (□), in the presence of melittin ($R_i = 15$). System were incubated 30 min above T_c and experiments performed on decreasing the temperature at a rate of 5° C/h. Melittin concentration is 0.35 mM. Gel-to-fluid phase transition temperatures for pure lipid systems are indicated by dashed vertical lines. Solid lines are drawn for eyeguide only.

T_c, increases when the acyl chain length increases. In addition to the large change already mentioned one detects, around T_c, small reproducible discontinuities which seem to increase as the chain length increases. When comparing the behaviour of DAPC-melittin with that of pure DAPC dispersions (not shown), one finds essentially the same intensity profile, i.e., a plateau below and above T_c linked by a steep increase in intensity on decreasing the temperature through T_c. The only variance residing in the small discontinuities which appear during the intensity increase, in the presence of melittin.

Experiments performed with higher melittin content ($R_i = 5$) on DPPC or DSPC membranes led to a complete abolition of the phase transition: the light scattered intensity reaches that observed at low temperatures. With DAPC membranes, for $R_i = 5$, curves are of the type already described for lower melittin content. Interestingly, a transient clearing is observed with DAPC, $R_i = 5$, when the temperature is decreased rapidly below T_c.

3.2. Quasi elastic light scattering

In order to quantitate light scattering changes described above, the size of the melittin-phosphatidylcholine systems has been determined as a function of lipid-to-peptide molar ratio and of temperature by QELS. In such a typical QELS experiment the system was first incubated above T_c at a given R_i for 30 min and then measurements were performed on decreasing the temperature at a rate of 10° C per h. The temperature variation of hydrodynamic radii hence obtained for DSPC-melittin exhibit profiles are very similar to those already described with static light scattering intensity measurements (Fig. 1), i.e., one observes a plateau of R_H on each side of T_c, at $R_i = 15$ (Fig. 2A), with a nearly 10-fold drop of the particle size on going below T_c. For higher doses of melittin, $R_i = 5$, the size transition disappears and the radius is almost constant ($R_H = 10$ nm) whatever the temperature (Fig. 2A). This behaviour strictly

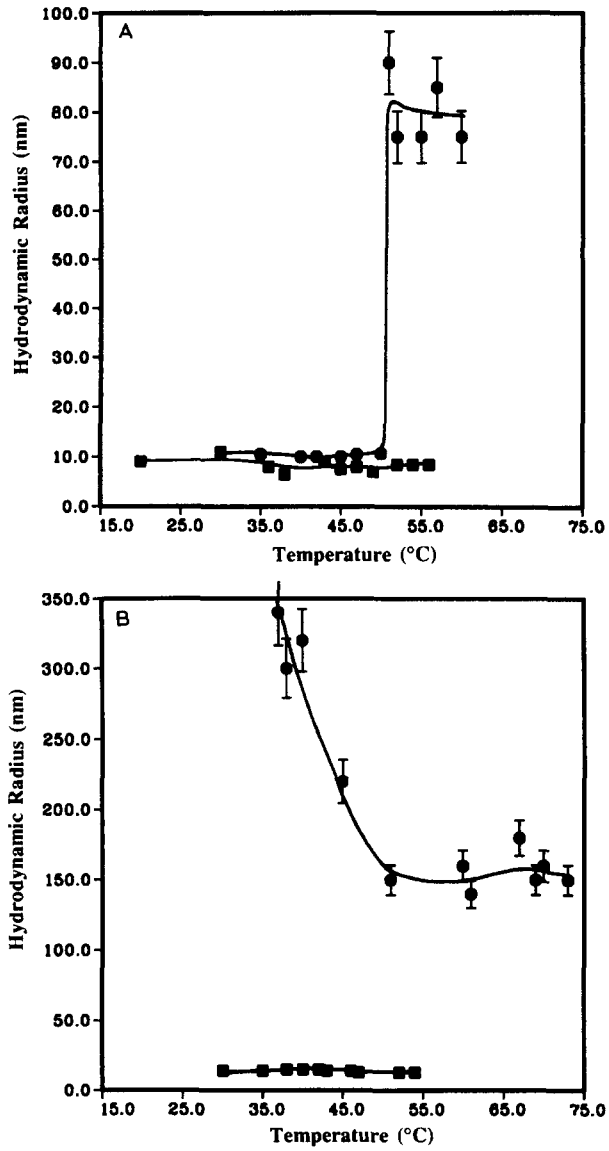

Fig. 2. Temperature variation of the hydrodynamics radius, R_H as measured by QELS. (A) DSPC-melittin, (●) $R_i = 15$, (■) $R_i = 5$. Temperature decrease at rate of 10° C per h. (B) DAPC-melittin, $R_i = 15$, (●) temperature decrease at a rate of 10° C per h, (■) temperature quench from the fluid phase in about 10 to 20 s. Solid lines are drawn for eyeguide only.

Table 1
Hydrodynamic radii, in nm, for DMPC-,DPPC-, DSPC- and DAPC-melittin systems at $R_i = 15$ and 5, in gel and fluid phase temperatures

System	Gel ($T - T_c = -11°$ C)		Fluid ($T - T_c = +9°$ C)	
	$R_i = 15$	$R_i = 5$	$R_i = 15$	$R_i = 5$
DMPC	7 *	n.d.	69 *	n.d.
DPPC	10	10	75	10
DSPC	10	10	90	10
DAPC	15 [a]	15 [a]	150	15 [b]

Accuracy is 10% except otherwise mentioned.
[a] Values obtained after temperature quench.
[b] Accuracy 30%.
* From [1].

parallels that of DPPC in the presence of melittin as already reported [1,3]. It must be emphasized here that the size of the multilamellar dispersions, in the absence of melittin, is of several hundred nm.

In the case of the DAPC-melittin system ($R_i = 15$) large vesicles of about 150 nm are observed in the fluid phase. When the temperature decreases from the fluid phase at rate of 10° C/h, as shown in Fig. 2B, there is no decrease in size associated with the transition temperature and for low temperatures (35° C), relative to T_c, the hydrodynamic radius increases up to 350 nm at 35° C. This behaviour is at variance to what has been observed with DPPC and DSPC but agrees very well with the light scattering profile of DAPC-melittin (Fig. 1). A totally different behaviour is observed if the same system is quenched from the fluid phase to temperatures in the gel phase of DAPC (Fig. 2B, lower curve). In these conditions, one observes a size transition, from large objects in the fluid phase to small structures in the gel phase, $R_H \sim 15$ nm, very similar to those detected with phosphatidylcholines of shorter chain length (Fig. 2A). Hydrodynamic radii both in gel and fluid phases are reported in Table 1 for the three systems. Data for DMPC-melittin system [1] has also been added to this table for comparison. For moderate amounts of Melittin, $R_i = 15$, one observes small structures (7–15 nm radius) below T_c and much larger objects (69–150 nm radius) above T_c. The size of objects depends on the lipid chain length: the longer the acyl chain the larger the hydrodynamic radius. Values reported herein for DPPC are in good agreement with those previously determined by QELS and electron microscopy [1].

3.3. Solid state ^{31}P-NMR

Dose–response effect of melittin on DPPC, DSPC and DAPC bilayers

In order to obtain more information about the conditions under which the small objects are formed phosphorus-31 NMR has been utilized. Fig. 3 shows the lineshape evolution of ^{31}P-NMR powder spectra for the three lipid systems, under progressive addition of melittin at temperatures where lipids are in their fluid phase ($T - T_c = +9°$ C). It must be emphasized that systems have been incubated in the fluid phase for 30 min prior the beginning of the NMR experiment. It can be noticed in this figure that for $R_i \geq 15$, spectra exhibit axially symmetric lineshapes characteristic of phosphorus-containing molecules undergoing axial reorientation as in a lamellar phase or in unilamellar vesicles of large radii. A small fraction of ($\leq 5\%$) isotropic line is also detected in such conditions and is attributed to a little phospholipid degradation (see Materials and methods). On the contrary, for $R_i < 15$, a sharp isotropic NMR line grows and dominates the spectra. Although such a line, in principle, can have various origins, its occurrence which strictly parallels the presence of very small objects (10–15 nm radius, Table 1), allows unambiguous attribution of this sharp NMR line to these small structures. It has indeed been shown by Burnell et al. [18] that axially symmetric powder patterns could be converted into isotropic lines if the curvature radius of spherical vesicles is small enough for the isotropic reorientation to averages to zero the residual ^{31}P chemical shift anisotropy. In Fig. 4 spectra are

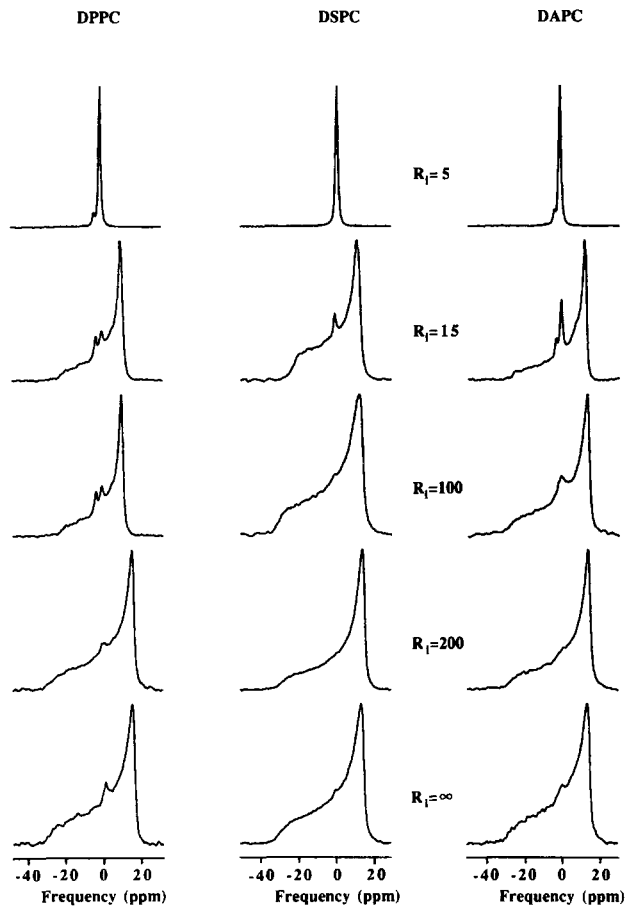

Fig. 3. Evolution of the DPPC, DSPC and DAPC ^{31}P-NMR powder spectra, in the fluid phase ($T - T_c = +9°$ C), under progressive addition of melittin. Experimental conditions: spectrometer frequency, 109.35 MHz; spectral window, 50 kHz; 90° pulse length, 8.6 μs; delay between the two pulses to form the echo 40 μs; 250 accumulations, 6 s recycling time; gated broad band proton decoupling. Phospholipid concentration, 50 mM.

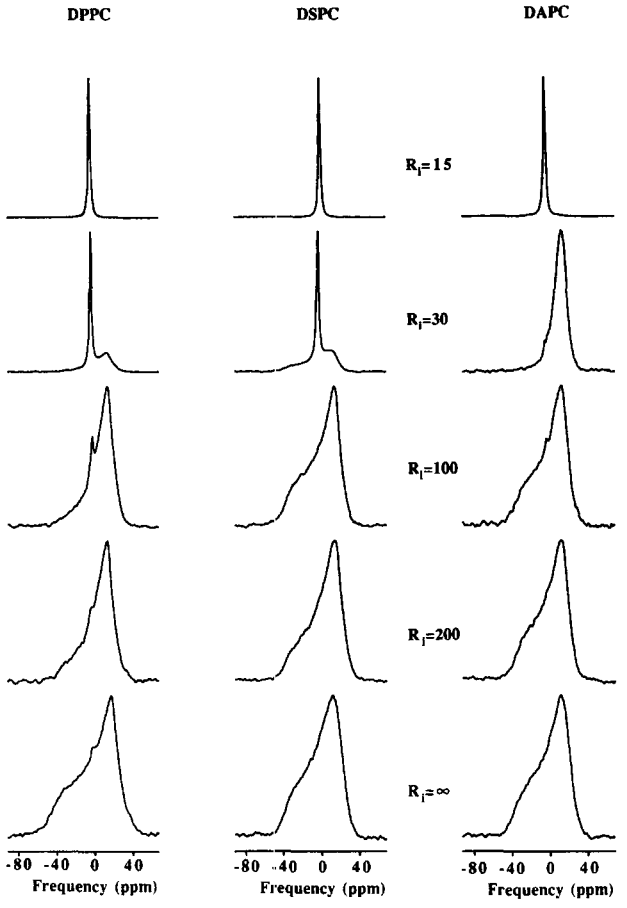

Fig. 4. Evolution of the DPPC, DSPC and DAPC ^{31}P-NMR powder spectra, in the gel phase ($T - T_c = -11°$ C) under progressive addition of melittin. Same experimental conditions as in Fig. 3. DAPC spectra are obtained under quenching conditions.

reported obtained versus R_i in the gel phase, at temperatures such that $T - T_c = -11°$ C. It must be reminded (Materials and methods) that systems were first prepared by incubation above T_c. Again, isotropic NMR lines appear when R_i decreases. However, these sharp lines are detected for higher R_i values, as compared with the fluid phase (Fig. 3), i.e., for lower doses of melittin in the system.

Calculation of the second moment of spectra allows to quantitative these spectral shape changes as shown on Fig. 5. The change from a powder pattern to a sharp isotropic line leads to a drastic decrease of the second moment by more than 2 orders of magnitude. It is remarkable that, for the three model membrane systems, a total conversion into an isotropic line occurs at the same melittin content, i.e., $R_i \approx 5$ in the fluid phase and $R_i \approx 15$ in the gel phase. This clearly indicates that the small melittin-lipid complexes are formed independently of chain length. This is in agreement with previous findings about melittin binding to DLPC, DMPC and DPPC [19]. Although the behaviour of the three systems described herein can be rationalized in the same manner, it must be recalled that low temperature melittin-DAPC spectra are observed under quenching conditions. It must be noted that in the case of the shorter chain lipid, DPPC, a small decrease in the second moment is detected in the gel phase at $R_i = 100$. The appearance of an isotropic line superimposed on a gel-type powder pattern correlates with the above observation but is not sufficient to account for the decrease in second moment observed at $R_i \approx 100$. A narrowing of the anisotropic spectra is also involved and indicates that the orientation and/or the dynamics of DPPC head groups are modified. A similar behaviour is also observed in the fluid phase. Here one notices a marked reduction of the chemical shift anisotropy for $15 \leq R_i \leq 100$. Since there is almost no isotropic line in these conditions, the tumbling of the large vesicles, as detected by QELS, must be in a time scale such that it leads to an additional averaging of the phosphate magnetic interaction.

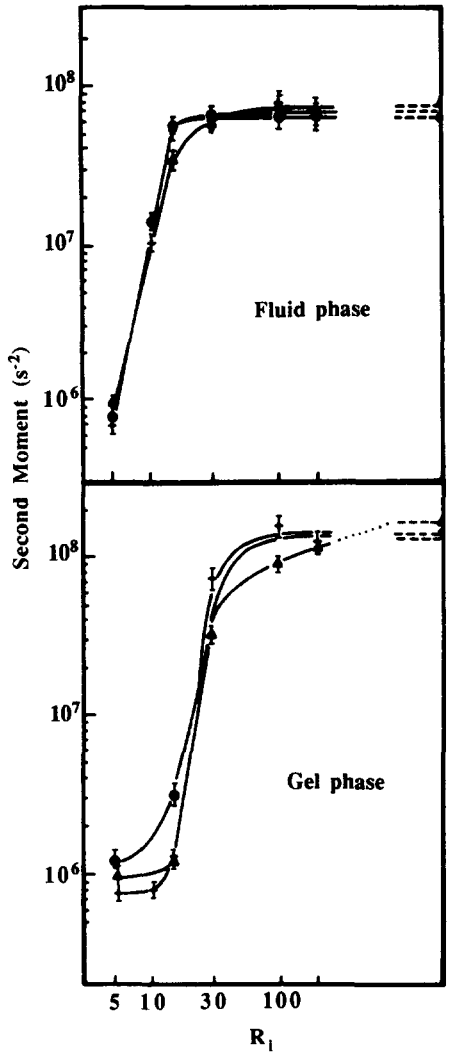

Fig. 5. Second moment of DPPC (▲), DSPC (+) and DAPC (●) ^{31}P-NMR spectra, as a function of the lipid-to-melittin molar ratio, R_i, in the gel ($T - T_c = -11°$ C) and fluid ($T - T_c = +9°$ C) phases. Solid lines are drawn for eyeguide only. Dashed lines indicate second moment values for pure systems.

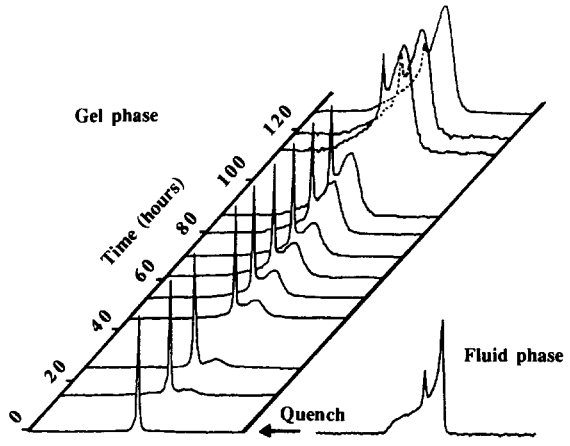

Fig. 6. Kinetics for evolution of DAPC ^{31}P-NMR spectra in the presence of melittin ($R_i = 15$), at $T - T_c = -11°$ C. The system has been quenched in a few seconds from the fluid phase ($T - T_c = 9°$ C). Time to record one spectrum is about 17 min. Same experimental conditions as in Fig. 3.

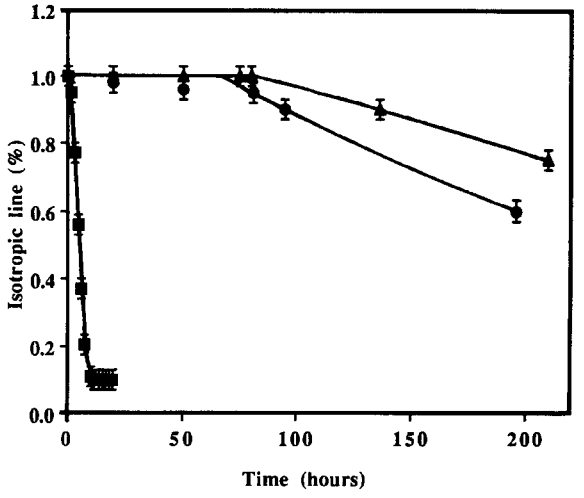

Fig. 7. Influence of lipid chain length on the kinetics of disappearance of the isotropic line for phosphatidylcholine-melittin ($R_i = 5$) systems, at $T - T_c = -11°$ C. All systems have been quenched from their respective fluid phase. DPPC (▲), DSPC (●) and DAPC (■). Solid lines are best fits according to a pseudo first order kinetic law (see text).

Long term stability of the small structures

As mentioned above, in the case of DAPC-melittin systems, small objects giving rise to isotropic NMR lines were obtained only under quenching conditions. This questions the stability of small objects in the gel phase. Experiments have thus been performed to monitor possible changes of the systems as a function of time following the quench. Fig. 6 illustrates such an evolution for DAPC-melittin ($R_i = 15$), at $T - T_c = -11°$ C, i.e., in the gel phase. Spectrum at time $t = 0$ is only constituted by an isotropic line, reflecting the presence of very small tumbling objects as already described by QELS. Successive spectra on the time-scale of hours shows that a broad component appears and increases as function of time. Intermediate spectra show the superimposition of an isotropic line on a powder pattern which indicate that there is slow exchange, in the ^{31}P-NMR time scale (milliseconds), of these two spectral features. For very long periods of time ($t = 130$ h), the isotropic line has almost totally disappeared and the observed powder pattern is very similar to that observed with lipid bilayers of very large sizes (several thousand Å curvature radius). Since all experimental NMR parameters are constant and since the absolute integrated area for each spectrum of Fig. 6 is constant, within the experimental error, spectral changes in this figure therefore reflect the variation of the respective populations of small and large objects. One may therefore integrate each subspectrum to determine the relative amounts of phospholipids in each macromolecular complex. Among several methods to do so, spectral simulations seem to be the most accurate. The spectral parameters needed to calculate both the isotropic and the powder subspectra are determined at once and kept constant for simulations of the entire series. In order to fit all spectra of Fig. 6, the relative amount of the time dependent signals (FIDs) giving rise to isotropic and powder patterns is varied. Fourier transformation of these signals leads to simulated spectra which are compared to experimental ones. Accuracy in the relative areas is within 5%. The disappearance of isotropic lines reflecting the instability of small objects can therefore be quantitized, as a function of time, and two parameters are shown to affect the stability: (i) the lipid acyl chain length and (ii) the temperature of the system.

The effects of the chain length on these kinetics is reported on the Fig. 7 for DPPC-, DSPC- and DAPC-melittin, $R_i = 5$, after temperature quench from the fluid phase to $T - T_c = -11°$ C. Such a low R_i has been chosen to limit experimental times. Dramatic differences in the behaviours of the three lipids are observed. Isotropic lines reflecting the presence of small objects appear to be very stable (up to several days) in the case of DPPC and DSPC whereas these lines disappear within a few hours with the longer chain length lipid DAPC. Findings with DPPC agree with a previous Raman study [5]. Moreover, it appears that isotropic lines observed with DPPC and melittin are detected in greater amounts, in the long term, than those observed with DSPC. The stability depends therefore on the acyl chain length and decreases in the sense: DAPC $\ll$ DSPC $<$ DPPC. Fig. 7 suggests that the process

Table 2
Kinetic parameters of disappearance of the isotropic NMR line for DPPC-, DSPC- and DAPC-melittin systems, in the gel phase, at $T - T_c = -11°$ C and $R_i = 15$

System	t_1 (h) [a]	R_f (h^{-1}) [b]
DPPC	80	$2 \cdot 10^{-3}$
DSPC	60	$4 \cdot 10^{-3}$
DAPC	1.5	$200 \cdot 10^{-3}$

[a] t_1 is the lag time after which the decrease of the isotropic line starts.
[b] R_f is the rate of fusion of the small discs (see text).

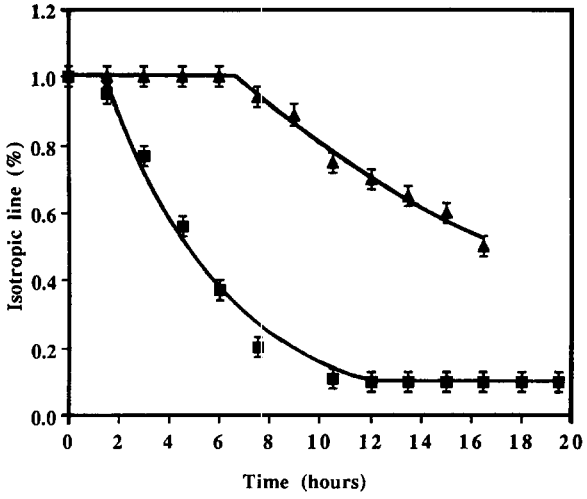

Fig. 8. Effect of temperature quench on the kinetics of disappearance of the isotropic line for the DAPC-melittin ($R_i = 5$) system. (■) $T - T_c = -11°$ C, (▲) $T - T_c = -17°$ C. Solid lines are best fits according to a pseudo-first-order kinetic law (see text).

may be pseudo-first-order of the form $p(t) = p_0 \exp(-(t - t_l)R_f) + p_\infty$ where p_0 and p_∞ are the proportions of isotropic line at $t = 0$ and ∞, respectively, and t_l the lag time before the decrease of isotropic line starts, $t - t_l = 0$ for $t \leq t_l$. In this equation $p(t)$ represents the area of isotropic line (the population of small objects) and R_f the rate associated with the fusion process. Table 2 summarizes results when applying this equation to the data of Fig. 7. It clearly appears that the rate of fusion of small objects made with DAPC is a lot higher than for systems made with shorter chain lipids.

Since the small objects are metastable at $T < T_c$, the conditions of temperature quench have been investigated. The Fig. 8 reports on the influence of the temperature jump, in the gel phase, on the kinetics of disappearance of the isotropic line, for DAPC-melittin ($R_i = 5$). When the system is quenched from the fluid phase to $T - T_c = -11°$ C or $T - T_c = -17°$ C, it is clearly noticed that the further away from the transition temperature the slower the isotropic line disappears. In addition one notices that the lag is of 1.5 h at $T - T_c = -11°$ C and of about 6 h at $T - T_c = -17°$ C. Although it is difficult to fit the data for $T - T_c = -17°$ C one can nonetheless remark that the rate of fusion decreases when decreasing the temperature in the gel phase.

Few experiments (not shown) have been performed to investigate on the influence of the amount of toxin on metastability. For $T - T_c = -11°$ C, it appears that fusion is much faster for $R_i = 5$ than for $R_i = 15$.

4. Discussion

The present work demonstrates that the vesicle-to-disc transition associated to the lipid chain melting already documented for DPPC-melittin systems [1,3,5] can be extended to longer chain lipids with a threshold for $C_{20:0}$ phosphatidylcholine chains. In addition, the conditions under which macromolecular changes occur and the stability of the newly formed structures are determined more accurately. As a general statement, it can be said that melittin similarly interacts with phosphatidylcholines, whatever the acyl chain length as was early recognized for DLPC, DMPC, DPPC [19]. This interaction leads to new lipid-toxin entities whose shape and size depend on temperature, relative to T_c, and on the amount of toxin. In the gel phase, small discoidal structures (lipid-toxin complexes) are formed. For $R_i > 15$, they coexist with large lamellar lipid structures not involved in the complex, whereas for $R_i \leq 15$, the system is totally converted into small species. Total transformation of the model membrane system into small discoids can be paralleled to a 'clearing' effect, melittin playing the role of a detergent-like molecule. The lipid-to-protein incubation ratio for which such a process is completed depends on the physical state of the lipids. Lipid dispersions in their gel phase are entirely converted into small discoids for $R_i \leq 15$ whereas greater amounts of toxin ($R_i \leq 5$) are needed to promote the same effect in fluid phase lipids. This is an indication that melittin preferentially solubilizes highly ordered lipids rather than fluid lipids. Entire membrane solubilization occurs for high amounts of toxin vs. lipids. However, the results presented herein show that the formation of small objects in the gel phase occurs even at very low amounts of toxin (e.g., $R_i = 100$ with DPPC). Moreover, their sizes appear to slightly depend, within the experimental error, on the acyl chain length. On the other hand, low concentrations of melittin in the fluid phase lead to large vesicles whose diameter increases as the chain length increases. In any case, melittin action implies restructuration of the lipid overall structure. If such processes were to occur in real membranes it would mean membrane lysis and death of the cell. Some recent evidences show that this could indeed be the case with human erythrocytes [8]. It is therefore important to understand the mechanisms of such processes.

Few data are available on the formation of the large vesicles in the fluid phase. It has been recognized that interaction of melittin with lipid lamellar phases is maximum in the fluid phase [11] and is a prerequisite for the formation of small discs in the gel phase. On the basis of ^{2}H-NMR data it has been proposed that melittin would insert in the membrane at high temperatures with respect to T_c and then go deeper into the bilayer core when decreasing the temperature towards T_c [2]. If melittin can be approximated to a rigid bent rod [20] and the lipids to much more dynamic species, this amphipathic cylinder could be expected to exert local mechanical constraints to the fluid bilayer leaflet. The latter will adapt itself to the constraint by local deformations allowed by the dynamic character of the lipid chains. Such deformations could lead

to impose a curvature radius to the bimolecular leaflet. It must be realized that such a result would requires some kind of cooperativity of the local constraints as already proposed by Battenburg et al. [21]. On the other hand, the increase in chain length is believed to increase the bilayer stability as a flat lamellae. Thus, the toxin mechanical constraint and the increase in chain length would have opposite effects. The chain accommodation in the fluid phase would nonetheless allow the formation of spheroidal vesicles whose radius increases with chain length. Fragmentation of these vesicles into small discoids is induced by cooling down the system below T_c. Such a process has already been discussed in the case of DPPC-melittin systems [1,3] and DMPC [22]: cooling the lipid-melittin complexes below T_c reduces considerably the lipid dynamics which can no longer accommodate for the mechanical constraint exerted by melittin. The system thus fragments into flat structures of smaller radius. As for DPPC, fusion of the small structures on increasing the temperature above T_c leads back to the large vesicles. The fusion-fragmentation mechanism allowing the size and shape transition of lipid-toxin complexes, and triggered by the order-disorder transition of pure lipids, appears therefore to be general for all saturated phosphatidylcholines investigated so far. Interestingly, the size of the small structures formed below T_c show little dependence on acyl chain length.

Small discs made up with melittin and DAPC are very hard to detect, one must quench the system below T_c whereas on the contrary, with DPPC and DSPC the discs occur readily whatever the way to pass through T_c. This can be understood on the basis of the model proposed by Dufourcq et al. [1]: some lipids would form the core of the small disc, the periphery of which being covered by melittin molecules. The hydrophobic side of the bent a helices must be in contact with the lipid acyl chains in order to maximize the amphipathic interactions thus lowering the free energy of the system. It could not be decided, from the available data, if the toxin molecules were perpendicular or parallel to the surface of the disc. However, on the basis of a lipid-to-toxin ratio of ca. 20–25 in the small structures, the position of melittin vertical to the disc plane was thought to be the most probable [1]. This model which has been called 'bicycle tire' by Segrest [23] in the case of apolipoproteins clearly shows what are the geometrical or mechanical constraints of the system. In order to get a stable particle in water, the length of the hydrophobic part of melittin (ca. 30 Å) must match the length of the lipid hydrophobic chain. One can estimate the length of DPPC apolar region to be ca. 30 Å in the gel phase, whereas that of DAPC would be ca. 40 Å. It is clear that the length of the DPPC acyl chains is matched properly by the length of the apolar residues (1–20) of melittin whereas the DAPC chains do not. The result of this mismatching would be to expose methylene groups to a polar medium, a situation highly unfavourable as far as the energy of the system is concerned. For intermediate chain length (i.e., C_{14} and C_{18}), the system may accommodate the mismatching by deformations of the disc to concave or convex forms. Such bilayer deformations have already been proposed by Bloom and Mouritsen [24] to account for certain type of lipid–protein interactions in membranes.

However, it must be emphasized that these lipid-toxin discs evolve in the long term towards extended bilayers. In other words, the small objects formed below T_c are metastable. This is not very surprising since it has been shown that melittin, when added directly to gel phase lipids does not promote any structural changes [2,11]. The equilibrium situation is therefore obtained when melittin is no longer associated with the hydrophobic core of gel phase lipids; however, melittin appears to stay in contact with the phosphate head group since perturbations in the chemical shielding anisotropy are still detected. The experiments presented herein show that the kinetics to reach this thermodynamic equilibrium depend upon the acyl chain length and the temperature of the system. The kinetic law involves a lag time during which the small objects are stable, followed by an exponential decrease of the amount of isotropic line (fusion of discs) as a function of time. The lag time increases and the rate of fusion decreases on decreasing the acyl chain length from C_{20} to C_{16} or on decreasing the temperature, relative to T_c.

5. Conclusion

The experiments presented herein allow to generalize the action of melittin on phosphatidylcholine model membranes. The bee venom toxin induces macroscopic bilayer restructuration for DPPC, DSPC and DAPC.

Formation of large vesicles with moderate to low amounts of toxin, in the fluid phase, fragmentation into small discoids when cooling down the system below T_c and relative stability of these discs in the gel phase can be accounted for by making use of a simple mechanistic model. Lipids and peptides can thus be described as having shapes able to exert mechanical constraints against each other, when associating together in a complex, as well as dynamical capabilities allowing then to adapt, to a certain extent, to the constraint exerted by other components. This allows the formation of new macromolecular entities, extending the already rich polymorphism of lipid phases.

The above description can lighten the mode of action of melittin on membranes. From the biological viewpoint, small discoids can be formed in the gel phase with very low amounts of toxin (e.g., $R_i = 100$ with DPPC). The action of melittin on real membranes can therefore be supposed to be akin to the direct lysis mechanism. This process involves bilayer restructuration and would therefore imply death of the cell. The data of Katsu and coworkers [10] which demonstrate that such peptides can, in parallel to hemolysis, partially solubilize lipids may be used to reinforce this conclusion. However, as already

mentioned long ago, it still remains to be proven that such a solubilization of natural membrane components is unrelated to a phospholipase activity.

References

[1] Dufourcq, J., Faucon, J.F., Fourche, G., Dasseux, J.L., Le Maire, M. and Gulik-Krzywicki, T. (1986) Biochim. Biophys. Acta 859, 33–48.
[2] Dufourc, E.J., Smith, I.C.P. and Dufourcq, J. (1986) Biochemistry 25, 6448–6455.
[3] Dufourc, E.J., Faucon, J.F., Fourche, G., Dufourcq, J., Gulik-Krzywicki, T. and Le Maire, M. (1986) FEBS Lett. 201, 205–209.
[4] Dufourcq, J., Dasseux, J.L. and Faucon, J.F. (1984) in Bacterial Protein Toxins (Alouf, J., Arbuthnott, J.P., Freer, J.F. and Fehrenbach, F.J., eds.), pp. 126–137, Academic Press, London.
[5] Lafleur, M., Dasseux, J.L., Pigeon, M., Dufourcq, J. and Pezolet, M. (1987) Biochemistry 26, 1173–1179.
[6] Dempsey, C.E. (1990) Biochim. Biophys. Acta 1031, 143–161.
[7] Batenburg, A.M., Hibbeln, J.C.L., Verkleij, A.J. and De Kruijff, B. (1987) Biochim. Biophys. Acta 903, 142.
[8] Dufourc, E.J., Bonmatin, J.M. and Dufourcq, J. (1989) Biochimie 71, 117–123.
[9] Katsu, T., Ninomiya, C., Kuroko, M., Kobayashi, H., Hirota, T. and Fujita, Y. (1988) Biochim. Biophys. Acta 939, 57–63.
[10] Katsu, T., Kuroko, M., Morikawa, T., Sanchika, K., Fujita, Y., Yamamura, H. and Uda, M. (1989) Biochim. Biophys. Acta 983, 135.
[11] Dasseux, J.L., Faucon, J.F., Lafleur, M., Pezolet, M. and Dufourcq, J. (1984) Biochim. Biophys. Acta 755, 37–50.
[12] Perly, B., Dufourc, E.J. and Jarrell, H.C. (1984) J. Label. Comp. Radiopharm. 21, 1–13.
[13] Faucon, J.F., Dufourcq, J., Lussan, C. and Bernon, B. (1976) Biochim. Biophys. Acta 436, 283–294.
[14] Mazer, N.A., Schurtenberger, P., Carey, M.C., Preisig, R., Weigand, K. and Känzig, W. (1984) Biochemistry 23, 1994–2005.
[15] Rance, M. and Byrd, R.A. (1983) J. Magn. Res. 52, 221–240.
[16] Abragam, A. (1961) Principles of Nuclear Magnetism, Oxford University Press, London.
[17] Marsh, D. (1990) CRC Handbook of Lipid Bilayers, CRC Press, Boca Raton, FL.
[18] Burnell, E.E., Cullis, P.R. and De Kruijff, B. (1980) Biochim. Biophys. Acta 603, 63–69.
[19] Dufourcq, J. and Faucon, J.F. (1977) Biochim. Biophys. Acta 467, 1–11.
[20] Eisenberg, D. (1984) Annu. Rev. Biochem. 53, 595.
[21] Batenburg, A.M., Van Esch, J.M. and De Kruijff, B. (1988) Biochemistry 27, 2324.
[22] Dempsey, C.E. and Sternberg, B. (1991) Biochim. Biophys. Acta 1061, 175–184.
[23] Segrest, J.P. (1977) Chem. Phys. Lipids 18, 7–22.
[24] Mouritsen, O.G. and Bloom, M. (1984) Biophys. J. 46, 141–153.